PHYSICAL REVIEW A **92**, 020502(R) (2015)

Single-photon excitation of $K\alpha$ in heliumlike Kr^{34+}: Results supporting quantum electrodynamics predictions

S. W. Epp,[1,*] R. Steinbrügge,[2] S. Bernitt,[2,†] J. K. Rudolph,[2,3] C. Beilmann,[4] H. Bekker,[2] A. Müller,[3] O. O. Versolato,[2] H.-C. Wille,[5] H. Yavaş,[5] J. Ullrich,[6] and J. R. Crespo López-Urrutia[2]

[1]*Max-Planck-Institut für Struktur und Dynamik der Materie, Luruper Chaussee 149, 22761 Hamburg, Germany*

[2]*Max-Planck-Institut für Kernphysik, Saupfercheckweg 1, 69117 Heidelberg, Germany*

[3]*Institut für Atom- und Molekülphysik, Justus-Liebig Universität Gießen, Leihgesterner Weg 217, 35392 Gießen, Germany*

[4]*Physikalisches Institut, Ruprecht-Karls-Universität Heidelberg, Im Neuenheimer Feld 226, 69120 Heidelberg, Germany*

[5]*Deutsches Elektronen-Synchrotron (PETRA III), Notkestraße 85, 22607 Hamburg, Germany*

[6]*Physikalisch-Technische Bundesanstalt (PTB), Bundesallee 100, 38116 Braunschweig, Germany*

(Received 15 May 2015; published 12 August 2015)

We study two fundamental transitions from the ground state $^1S_0$ to $^1P_1$ (w line) and $^3P_1$ (y line) in heliumlike Kr^{34+} by resonant single-photon excitation using an electron-beam ion trap and monochromatic x rays at PETRA III. Our results for the transition energies $E(w) = 13\,114.47(14)$ eV and $E(y) = 13\,026.15(14)$ eV are in excellent agreement with quantum electrodynamics calculations, but disagree for w with the average of the hitherto reported experimental results $\overline{E}_{\mathrm{Lit}}(w) = 13\,115.15(17)$ eV. Independently of any energy calibration, we obtain a value $E(w)/E(y) = 1.006\,780(7)$, also in consistency with predictions.

DOI: 10.1103/PhysRevA.92.020502 PACS number(s): 32.30.Rj, 12.20.Fv, 31.30.jf, 32.50.+d

Three-body systems such as heliumlike ions are cornerstones for atomic structure theory. Presently, quantum electrodynamics (QED) gives the most comprehensive interpretation of the electromagnetic interaction and provides the highest predictive accuracy in physics [1–7]. However, levels of highest precision have been exclusively achieved in comparatively light atoms or ions, where electrons are bound by rather weak Coulomb fields mediated by a low-Z nucleus. Here, QED calculations are usually realized by means of perturbation theory with small expansion parameters α and αZ, where α denotes the fine-structure constant and Z the atomic number. For high-Z systems, however, the expansion parameter αZ cannot be considered small and therefore more complex, nonperturbative methods developed in the last decades are required [8–17]. Experimentally, the spectroscopy of heavy few-electron systems, with low interelectronic correlation contributions, has advanced accordingly [18]. Recent results [19,20] concerning the proton size determination utilizing the spectroscopy of muonic atoms have raised the question of unaccounted-for QED contributions as a possible solution to the existing discrepancies to electron-scattering data and hydrogen results. In this light, accurate studies of highly charged ions, where the size of the $1s$ orbital can be comparable to the $2s$ orbital typically probed in muonic hydrogen, are valuable for complementary tests of QED.

In this Rapid Communication we investigate two prominent ground-state transitions in heliumlike Kr^{34+} by resonant photon excitation at about 600 times higher photon energy than in neutral helium [21] and double the energy than in a recent Fe^{24+} [22] measurement. The two lines investigated are the $1s^2\ ^1S_0 \rightarrow 1s2p\ ^1P_1$ and the $1s^2\ ^1S_0 \rightarrow 1s2p\ ^3P_1$ transitions, denoted in the literature as the w line and the y line, respectively. An improved value for the w transition energy in heliumlike Kr^{34+} is particularly important for settling a recent controversy concerning a deviation of presently available experimental data from QED calculations [23–25]. We compare our results with existing measurements and with available predictions, including a second-order QED approach [26] as well as a relativistic configuration interaction and perturbative many-body formulations [27,28]. Given uncertainties refer to one-sigma standard deviations throughout this Rapid Communication.

While there exists a rich literature of experimental work on y and w in heliumlike ions at low and mid Z values, the three heaviest elements investigated are Kr^{34+} [32–36], Xe^{52+} [37,38], and U^{90+} [39]. Compared to these experiments, our current relative accuracy is two to 30 times higher. We employ an original method [22,40–42] for the spectroscopy of highly charged ions (HCIs) analogous to single-photon laser spectroscopy but extended to x-ray energies of 13 keV. The technique is based on combining an electron-beam ion trap (EBIT) with advanced light sources such as third-generation storage rings [22,41] or free-electron lasers [40,42,43].

The experiments were performed at the P01 beamline of the PETRA III facility at DESY. We employed FLASH-EBIT [43] for generating and trapping a dilute cloud of heliumlike krypton. The arrangement is similar to earlier reports by us [22,42,43]. Basically, the FLASH-EBIT employs a continuous electron beam of up to 0.5 A current with sufficient kinetic energy to ionize the target ions. At the same time, the beam represents a negative line charge capable of trapping positive ions. Several 10^6 ions are contained within a cloud of 50 mm length and about 200 μm diameter.

For the measurement we collinearly overlap a monochromatic photon beam [size about $(200 \times 500)\ \mu m^2$] with the cylindrical ion cloud, and tune its energy across the transitions of interest. The fluorescence decay following excitation is recorded by means of a germanium detector [22] as a function of the photon beam energy. Up to about 35 counts per

*Corresponding author: sepp@mpsd.mpg.de

†Present address: Institut für Optik und Quantenelektronik, Friedrich-Schiller-Universität Jena, Max-Wien-Platz 1, 07743 Jena, Germany.

TABLE I. Measured Bragg angles, energies for w, y, and distinct absorption features. Column two gives the number of individual measurements per feature. Column three lists the least-square raw angles determined in Si(111) and Si(333) reflection. Column four gives the refraction and angle-offset $\epsilon_{\mathrm{exp,i}}$ corrected Bragg angles. In columns five and six the determined angle offset ϵ_{exp} and the wavelength-dependent refractive index n as $1-n$ are listed. Columns seven and eight display the x-ray energy of each feature as determined by using $a_{\mathrm{Si}}(y) = 5.430\,297(17)$ Å and $a_{\mathrm{Si}}(\mathrm{Pb}) = 5.430\,280(38)$ Å, respectively. The last column lists the theoretical results from Ref. [26] and the last row the energy ratio (dimensionless) obtained with Si(333).

Feature	Scans	θ_{exp} (deg)	θ_{B} (deg)	$10^5\epsilon_{\mathrm{exp,i}}$ (deg)	$1-n$ (ppm)	$E[a_{\mathrm{Si}}(y)]$ (eV)	$E[a_{\mathrm{Si}}(\mathrm{Pb})]$ (eV)	E_{theory} (eV)
y line (111)	7	8.731791(36)	8.730930(120)	26(6)	2.87(30)		13026.24(23)	13026.1165(41)
w line (111)	21	8.672611(19)	8.671750(120)	15(4)	2.83(30)		13114.44(23)	13114.4705(41)
$\mathrm{Se}^1_{\mathrm{edge}}(111)$	2	8.985640(70)	8.984750(130)	34(17)	3.04(30)		12661.14(23)	
$\mathrm{Se}^2_{\mathrm{edge}}(111)$	2	8.988610(70)	8.987710(130)	0(18)	3.04(30)		12657.00(23)	
y line (333)	25	27.08983(8)	27.08978(9)	26(6)	2.87(30)	13026.12(4)	13026.15(14)	13026.1165(41)
w line (333)	12	26.89264(6)	26.89258(8)	15(4)	2.83(30)	13114.44(4)	13114.47(14)	13114.4705(41)
$\mathrm{Se}^1_{\mathrm{edge}}(333)$	2	27.93835(35)	27.93830(35)	34(17)	3.04(30)		12660.98(19)	
$\mathrm{Se}^2_{\mathrm{edge}}(333)$	2	27.94755(36)	27.94750(36)	0(18)	3.04(30)		12657.15(20)	
$\mathrm{Pb}^*_{\mathrm{edge}}(333)$	2	27.02935(20)	27.02930(21)		2.86(30)		13053.10(10)	
$E^{333}(w)/E^{333}(y)$						1.006780(7)	1.006780(7)	1.0067828(4)

second into the 10 cm^2 sensitive detector area are recorded. We employ a double-crystal, high-heat-load monochromator (HHLM) [44] equipped with a Si(111)-cut crystal pair reaching at 13 keV photon energy a resolving power $E/\Delta E = 6500$ in first diffraction order and $E/\Delta E = 120\,000$ for the Si(333) plane reflections.

To determine the energy (or wavelength) of the w and y line we basically take the measured angles and apply Bragg's law for the diamond-cubic crystal structure of silicon,

$$\lambda^2 = \frac{4a_{\mathrm{Si}}^2 \sin^2(\theta_{\mathrm{B}})}{h^2+k^2+l^2}, \tag{1}$$

where λ denotes the wavelength, a_{Si} stands for the lattice constant of silicon, θ_{B} is the Bragg angle, and h,k,l (in this Rapid Communication, $h = k = l$, $h = 1$, or $h = 3$) are the Miller indices of the reflecting plane. The use of Eq. (1) has two important constraints: First, it requires absolute values for the angles, and second, the experimental angles need to be corrected for refraction. Within such an evaluation, corrections derived from the kinematical theory [45] provide sufficient accuracy. We find $n < 1$ for the refractive index of Si at the relevant x-ray energies and correct for a wavelength shift of the x rays entering the crystal and also for deviations in the angle of incidence according to Snell's law. Simple geometrical considerations in analogy to Ref. [46] lead to an expression for the measured θ_{exp} and the true, not directly observable, Bragg angle θ_{B}, which fulfills Bragg's condition inside the crystal:

$$\theta_{\mathrm{B}} - \theta_{\mathrm{exp}} - \epsilon_{\mathrm{exp}} = \left(\frac{1}{n}-1\right)[\tan(\theta_{\mathrm{exp}}+\epsilon_{\mathrm{exp}})+\tan(\theta_{\mathrm{exp}}+\epsilon_{\mathrm{exp}}+\alpha_{\mathrm{Si}})]. \tag{2}$$

Here, the parameter ϵ_{exp} denotes an initially unknown shift of the HHLM encoder angular scale from the absolute angles. The parameter α_{Si} represents a potential misalignment ω ($\alpha_{\mathrm{Si}} = 90^\circ - \omega$) of the surface of the crystal with respect to the (111) planes due to the crystal manufacturing. The experiment is insensitive to any reasonably expectable miscut, nonetheless we conservatively estimate a value $\alpha_{\mathrm{Si}} = 90^\circ \pm 0.1^\circ$. Extrapolation of data presented in Refs. [47,48] provides values for the refractive index n in the energy range around 13 keV (see Table I). Adjusting the Bragg angle is basically done by rotating the crystal pair. The unknown parameter ϵ_{exp} in Eq. (2) has to be determined before applying a correction to the measured angles θ_{exp}. If two diffraction orders, e.g., Si(111) and Si(333), are used to determine each transition, we can connect them via Eq. (1):

$$\sin\left(\theta_{\mathrm{B}}^{111}\right) = \frac{\sin\left(\theta_{\mathrm{B}}^{333}\right)}{3}. \tag{3}$$

In order to enhance the statistical basis we do not only solve Eq. (3) for the angles found for the transitions w and y, but also for the angles evaluated for two distinct features ($\mathrm{Se}^1_{\mathrm{edge}}$,$\mathrm{Se}^2_{\mathrm{edge}}$) [49] in the K-shell absorption edge of selenium. For this purpose we employed two photodiodes measuring the photon flux before and after the 37 μm Se foil, which was mounted between the HHLM and the FLASH-EBIT. We thus obtain four equations of type (3), each with a corresponding equation analogous to Eq. (2). These pairs of equations are solved simultaneously to get a corresponding $\epsilon_{\mathrm{exp,i}}$ (see the fifth column in Table I). The four $\epsilon_{\mathrm{exp,i}}$ values are combined by a least-square fit to infer the best value $\epsilon_{\mathrm{exp}} = (1.8 \pm 0.4) \times 10^{-4}$ deg used for the correction of the raw angle data of Table I by means of Eq. (2). A Gaussian function is fitted to each individual resonance to obtain the center-of-gravity Bragg angle (CBA). In a second step, the various CBAs are statistically combined to determine the least-square value for each feature in each order (see the third column in Table I). As an example, the raw data of a single scan (out of a total of 12) of the w line are depicted in Fig. 1. The spectra exhibit a very low background and are not blended by any other lines. Due to the five times smaller transition probability of the y transition, a longer integration is needed and a flat background, subtracted in Fig. 1, of about 73 counts occurs.

Calculating the wavelengths from the Bragg angles requires knowledge of the lattice constant a_{Si}. Although its nominal value is known to 5 parts per 10^9 (ppb) [50], we need to consider its temperature dependence [51]. At the time of the experiment we had no access to temperature information of

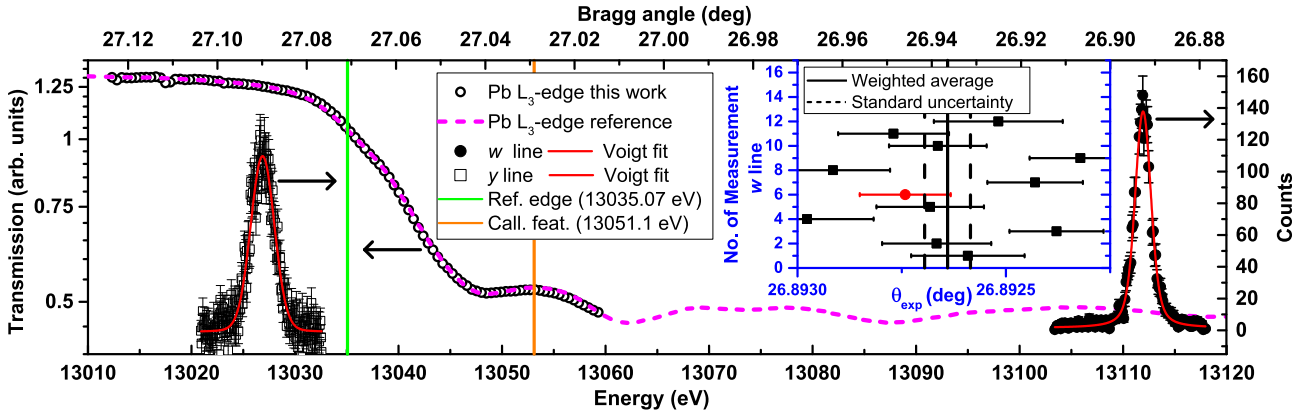

FIG. 1. (Color online) Experimental raw data [Si(333)] of the w and y line along with the Pb L_3-edge absorption spectrum (PbL) for energy calibration. The w data points show a result from a single scan (No. 6 data point in red) lasting about 15 min. A Gaussian fit to this scan provides a reduced chi-squared (RCS) of 1.3 and a center Bragg angle of $\theta_{\rm exp} = 26.892\,74(4)^\circ$. A Voigt fit, as depicted, produces even more favorable RCSs. The y line data represent an overlay of 25 single scans (background of 73 counts subtracted). The PbL (open circles) shows our data scaled to the (dashed) reference data [29–31]. Inset (blue): Centroids from 12 individual scans of w. Error bars include counting statistics, angular encoder errors (1 ppm), and errors due to normalization to the ion fill factor of the trap and beam overlap mismatch (~3 ppm).

the cryocooled crystals. By a future determination of this temperature, the x-ray wavelengths will be traceable to the System of Units (SI) via the lattice spacing of the Si crystal. Here, we determine the value of $a_{\rm Si}$ by cross calibrating our angular scale by means of known wavelengths. For this we apply two methods: First, we take the known photon-energy dependence of the absorption edge of the L shell of lead leading to $a_{\rm Si}$(Pb), and second, for comparison, we calibrate our experimental y line in third order using the theoretical value of Artemyev *et al.* [26] giving $a_{\rm Si}(y)$.

Obviously, the second procedure does not allow one to absolutely test theory. Nevertheless, using $a_{\rm Si}(y)$ and taking the values of order Si(333) from the seventh column of Table I, we find for the energy of the w line a deviation of below 0.04 eV or 3 ppm in comparison to the theoretical prediction [14] (ninth column of Table I). This remarkable agreement challenges recent suspicions of a general, systematic Z-dependent deviation [23] between theory and experiment claimed to be of about 0.3 eV for Kr. The consistency we find at the given accuracy basically leaves us with the common ground state of w and y as the only remaining potential source for an energy shift of the size anticipated in Ref. [23]. To exclude that, an absolute energy calibration is necessary.

Our absolute energy values are determined by calibrating the angular scale utilizing the absorption features around the Pb L_3 edge. This procedure is analogous to the one described for the Se K edge. The Pb L_3 edge offers an energy accuracy of up to 2 ppm following the procedure reported in Ref. [29]. To improve our calibration accuracy we do not use the asymmetrically shaped absorption edge at 13 035.07 eV as defined in the original work of Kraft *et al.* [29], but instead a more symmetric feature $\rm Pb^*_{edge}$ also found in the original data [30,31] at 13 053.1 eV that is not explicitly mentioned in Ref. [29]. This feature is less prone to shifts in position that result from changes in the energy spread of the monochromatic beam. Shifts of the edge position depending on the resolution of the probing beam are a known problem [29,52]. Our transmission curve is plotted in Fig. 1, together with the reference data. The nominal edge position and our calibration feature are both indicated. We conservatively set an uncertainty of 0.1 eV for the literature reference energy of our Pb calibration feature. That is about three times larger than the one reported [29] for the neighboring absorption edge itself and accounts for the difficulties [52] potentially attached in comparisons of edge data, such as the chemical composition of the sample. With this method we deduce a lattice constant $a_{\rm Si}$(Pb) = 5.430 280(38) Å along with corresponding transition energy values (eighth column of Table I).

Although we obtain a calibration simultaneously valid for both the first and the third order, we use the Si(333) values because they are less susceptible to corrections by refraction or angle offset. Moreover, the energy calibration was carried out in third diffraction order. Our absolutely calibrated energy values, plotted in Fig. 2, are $E(y) = 13\,026.15(14)$ eV

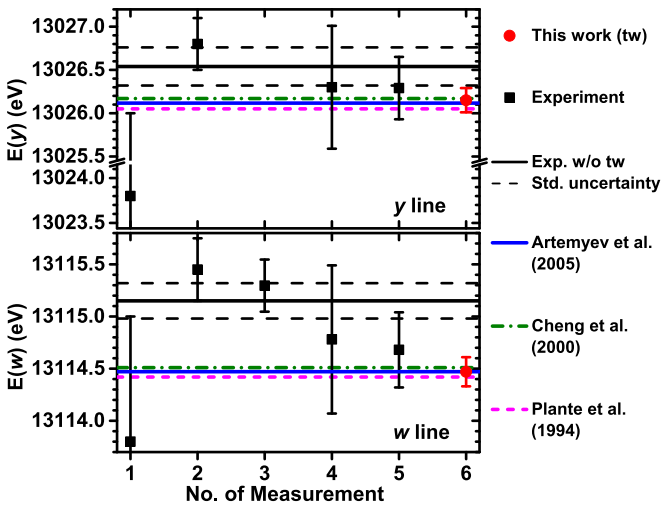

FIG. 2. (Color online) Comparison of our w and y line results with available theoretical and experimental values. Measurements No. 1 to No. 5 indicate results from Refs. [32–36], respectively. The black solid line is the weighted average of measurements No. 1 to No. 5. Theoretical data from Artemyev *et al.* [26], Cheng *et al.* [27], and Plante *et al.* [28] are included.

TABLE II. Budget of uncertainties U_i for the absolute values of $E(y)$ and $E(w)$ in eV determined in order Si(333) [generally larger for Si(111)]. Type (A) uncertainties arise from random, statistical effects while type (B) is not of type (A), e.g., resulting from systematic effects. U_1 arises from the experimental angle data including fit statistics, beam pointing, and statistical encoder errors. A systematic, but angle-independent, error of the encoder would cancel out due to the combined use of at least two different orders of diffraction.

	U_i [$E(y)$]	U_i [$E(w)$]
(1) Bragg angle $\theta_{\rm exp}$ (A)	0.03	0.02
(2) Angle offset ϵ (A)	<0.01	<0.01
(3) Refractive index n (B)	0.02	0.02
(4) Miscut α ($\pm 0.1^\circ$) (B)	<0.01	<0.01
(5) Lit. calibration energy (B)	0.10	0.10
(6) This work expt. edge data ($\theta_{\rm exp}$) (A)	0.09	0.09
Combined (quadratically)	0.14	0.14

and $E(w) = 13\,114.47(14)$ eV, with approximately 11 ppm relative combined standard uncertainty. We find excellent agreement with current theory and several hitherto reported experimental values [32,35,36] for both transitions, particularly confirming earlier EBIT results [36]. Our energy for the w transition differs significantly from two existing experimental reports [33,34] as well as the weighted average of the reported literature results $\overline{E}_{\rm Lit}(w) = 13\,115.15(17)$ eV as the two-sigma uncertainty intervals do not overlap. In the case of the y line, the discrepancy to other experiments is less pronounced and essentially within statistical limits.

We reach an enhanced relative accuracy of 7 ppm for the result $E(w)/E(y) = 1.006\,780(7)$, which is the energy of $E(w)$ in units of $E(y)$. This is possible since our method provides the direct relation between different orders of diffraction [Eq. (1)], resulting in an inherent energy calibration in units of a recorded transition. Linking this internal energy scale to the electron volt can be accomplished without the use of any calibration feature [53,54] if the temperature dependent lattice constant of the Si crystal is known.

Table II lists the relevant contributions to our uncertainty budget, which is dominated by that of the Pb edge calibration with 0.09 eV uncertainty in our experimental edge data and 0.1 eV attributed to the reference energy [29]. Our relative results found by using the independently determined $a_{\rm Si}(y)$ and also the energy ratio exhibit smaller uncertainties, partly since some systematic uncertainties approximately cancel. The largest unaccounted source of uncertainty is a potential crystal temperature difference between the first and third order of reflection caused by different efficiencies in absorption and reflection of the intense x-ray beam under different crystal angles. The effect could result in an apparent lattice constant $a_{\rm Si}$ which is angle dependent. Within the same order of diffraction, y, w, and $\rm Pb^*_{edge}$ are within 0.1° and cannot be affected noticeably at the present level of accuracy. The effect is largest between two different orders of diffraction. However, its influence is small as long as the calibration lines in close proximity to the measurement transitions are used, as is the case here.

In summary, we find a different value for the energy $E(w) = 13\,114.47(14)$ eV that is inconsistent with the weighted average value of experimental results reported so far, but in full agreement with the most advanced theoretical predictions. Our measured w line transition energy defies the recent claim of a general Z-dependent divergence between theory and experiment by Chantler *et al.* [23].

With our approach of resonant single-photon excitation spectroscopy deep in the x-ray range, we open the door to future sub-ppm spectroscopy in highly charged ions, benchmarking strong-field QED. As a next step, we plan on adding a second channel-cut crystal monochromator to the setup. This will significantly increase the achievable energy resolution and provide the capability for linking x-ray transition energies without the need for primary calibration lines to the silicon lattice constant at a nominal temperature, and hence to a SI-defined standard. The symmetric resonant transitions in such HCI will provide accurate x-ray energy standards [55] in future experiments.

We thank U. Kuetgens (Physikalisch-Technische Bundesanstalt) for making available the original data sets from Ref. [29].

[1] M. Niering, R. Holzwarth, J. Reichert, P. Pokasov, T. Udem, M. Weitz, T. W. Hänsch, P. Lemonde, G. Santarelli, M. Abgrall *et al.*, Phys. Rev. Lett. **84**, 5496 (2000).
[2] U. Jentschura, S. Kotochigova, E.-O. Le Bigot, P. Mohr, and B. Taylor, Phys. Rev. Lett. **95**, 163003 (2005).
[3] C. G. Parthey, A. Matveev, J. Alnis, B. Bernhardt, A. Beyer, R. Holzwarth, A. Maistrou, R. Pohl, K. Predehl, T. Udem *et al.*, Phys. Rev. Lett. **107**, 203001 (2011).
[4] S. Sturm, A. Wagner, B. Schabinger, J. Zatorski, Z. Harman, W. Quint, G. Werth, C. H. Keitel, and K. Blaum, Phys. Rev. Lett. **107**, 023002 (2011).
[5] K. Pachucki, U. Jentschura, and V. A. Yerokhin, Phys. Rev. Lett. **93**, 150401 (2004).
[6] D. Hanneke, S. Fogwell, and G. Gabrielse, Phys. Rev. Lett. **100**, 120801 (2008).
[7] T. Aoyama, M. Hayakawa, T. Kinoshita, and M. Nio, Phys. Rev. Lett. **99**, 110406 (2007).
[8] V. Shabaev, Phys. Rep. **356**, 119 (2002).
[9] I. Lindgren, S. Salomonson, and B. Åsén, Phys. Rep. **389**, 161 (2004).
[10] P. Mohr, Ann. Phys. (NY) **51**, 26 (1974).
[11] P. J. Mohr, Phys. Rev. Lett. **34**, 1050 (1975).
[12] P. J. Mohr, G. Plunien, and G. Soff, Phys. Rep. **293**, 227 (1998).
[13] S. A. Blundell, P. J. Mohr, W. R. Johnson, and J. Sapirstein, Phys. Rev. A **48**, 2615 (1993).
[14] P. Indelicato and P. J. Mohr, Phys. Rev. A **63**, 052507 (2001).
[15] H. Persson, S. Salomonson, P. Sunnergren, and I. Lindgren, Phys. Rev. Lett. **76**, 204 (1996).
[16] H. Persson, I. Lindgren, L. N. Labzowsky, G. Plunien, T. Beier, and G. Soff, Phys. Rev. A **54**, 2805 (1996).

[17] I. Lindgren, H. Persson, S. Salomonson, and L. Labzowsky, Phys. Rev. A **51**, 1167 (1995).
[18] P. Beiersdorfer, J. Phys. B **43**, 074032 (2010).
[19] R. Pohl, A. Antognini, F. Nez, F. D. Amaro, F. Biraben, J. M. R. Cardoso, D. S. Covita, A. Dax, S. Dhawan, L. M. P. Fernandes *et al.*, Nature (London) **466**, 213 (2010).
[20] A. Antognini, F. Nez, K. Schuhmann, F. D. Amaro, F. Biraben, J. M. R. Cardoso, D. S. Covita, A. Dax, S. Dhawan, M. Diepold *et al.*, Science **339**, 417 (2013).
[21] K. S. E. Eikema, W. Ubachs, W. Vassen, and W. Hogervorst, Phys. Rev. Lett. **71**, 1690 (1993).
[22] J. K. Rudolph, S. Bernitt, S. W. Epp, R. Steinbrügge, C. Beilmann, G. V. Brown, S. Eberle, A. Graf, Z. Harman, N. Hell *et al.*, Phys. Rev. Lett. **111**, 103002 (2013).
[23] C. T. Chantler, M. N. Kinnane, J. D. Gillaspy, L. T. Hudson, A. T. Payne, L. F. Smale, A. Henins, J. M. Pomeroy, J. N. Tan, J. A. Kimpton *et al.*, Phys. Rev. Lett. **109**, 153001 (2012).
[24] S. W. Epp, Phys. Rev. Lett. **110**, 159301 (2013).
[25] C. T. Chantler, M. N. Kinnane, J. D. Gillaspy, L. T. Hudson, A. T. Payne, L. F. Smale, A. Henins, J. M. Pomeroy, J. A. Kimpton, E. Takacs *et al.*, Phys. Rev. Lett. **110**, 159302 (2013).
[26] A. N. Artemyev, V. M. Shabaev, V. A. Yerokhin, G. Plunien, and G. Soff, Phys. Rev. A **71**, 062104 (2005).
[27] K. T. Cheng and M. H. Chen, Phys. Rev. A **61**, 044503 (2000).
[28] D. R. Plante, W. R. Johnson, and J. Sapirstein, Phys. Rev. A **49**, 3519 (1994).
[29] S. Kraft, J. Stumpel, P. Becker, and U. Kuetgens, Rev. Sci. Instrum. **67**, 681 (1996).
[30] S. Kraft, Ph.D. thesis, Universität Braunschweig, Germany, 1995.
[31] U. Kuetgens (private communication).
[32] J. P. Briand, M. Tavernier, R. Marrus, and J. P. Desclaux, Phys. Rev. A **29**, 3143 (1984).
[33] P. Indelicato, J. P. Briand, M. Tavernier, and D. Liesen, Z. Phys. D **2**, 249 (1986).
[34] E. V. Aglitsky, P. S. Antsiferov, S. L. Mandelstam, A. M. Panin, U. I. Safronova, S. A. Ulitin, and L. A. Vainshtein, Phys. Scr. **38**, 136 (1988).
[35] K. Widmann, P. Beiersdorfer, and V. Decaux, Nucl. Instrum. Methods Phys. Res., Sect. B **98**, 45 (1995).
[36] K. Widmann, P. Beiersdorfer, V. Decaux, and M. Bitter, Phys. Rev. A **53**, 2200 (1996).
[37] J. P. Briand, P. Indelicato, A. Simionovici, V. S. Vicente, D. Liesen, and D. Dietrich, Europhys. Lett. **9**, 225 (1989).
[38] D. B. Thorn, M. F. Gu, G. V. Brown, P. Beiersdorfer, F. S. Porter, C. A. Kilbourne, and R. L. Kelley, Phys. Rev. Lett. **103**, 163001 (2009).
[39] J. P. Briand, P. Chevallier, P. Indelicato, K. P. Ziock, and D. D. Dietrich, Phys. Rev. Lett. **65**, 2761 (1990).
[40] S. W. Epp, J. R. Crespo López-Urrutia, G. Brenner, V. Mäckel, P. Mokler, R. Treusch, M. Kuhlmann, M. Yurkov, J. Feldhaus, J. Schneider *et al.*, Phys. Rev. Lett. **98**, 183001 (2007).
[41] M. C. Simon, J. R. Crespo López-Urrutia, C. Beilmann, M. Schwarz, Z. Harman, S. W. Epp, B. L. Schmitt, T. M. Baumann, E. Behar, S. Bernitt *et al.*, Phys. Rev. Lett. **105**, 183001 (2010).
[42] S. Bernitt, G. V. Brown, J. K. Rudolph, R. Steinbrügge, A. Graf, M. Leutenegger, S. W. Epp, S. Eberle, K. Kubiček, V. Mäckel *et al.*, Nature (London) **492**, 225 (2012).
[43] S. W. Epp, J. R. Crespo López-Urrutia, M. C. Simon, T. Baumann, G. Brenner, R. Ginzel, N. Guerassimova, V. Mäckel, P. H. Mokler, B. L. Schmitt *et al.*, J. Phys. B **43**, 194008 (2010).
[44] J. Horbach, M. Degenhardt, U. Hahn, J. Heuer, H. Peters, H. Schulte-Schrepping, A. Donat, and H. Lüdecke, Nucl. Instrum. Methods Phys. Res., Sect. A **649**, 136 (2011).
[45] P. P. Ewald, Acta Crystallogr., Sect. A: Found. Crystallogr. **50**, 411 (1986).
[46] A. J. C. Wilson and W. L. Bragg, Math. Proc. Cambridge Philos. Soc. **36**, 485 (1940).
[47] M. Deutsch and M. Hart, Phys. Rev. B **37**, 2701 (1988).
[48] M. Deutsch and M. Hart, Phys. Rev. B **30**, 640 (1984).
[49] A local minimum and maximum in the transmission versus Bragg angle spectrum. See also Table I.
[50] E. Massa, G. Mana, U. Kuetgens, and L. Ferroglio, New J. Phys. **11**, 053013 (2009).
[51] K. G. Lyon, G. L. Salinger, C. A. Swenson, and G. K. White, J. Appl. Phys. **48**, 865 (1977).
[52] R. Deslattes, E. Kessler, P. Indelicato, L. de Billy, E. Lindroth, and J. Anton, Rev. Mod. Phys. **75**, 35 (2003).
[53] P. Amaro, S. Schlesser, M. Guerra, E.-O. Le Bigot, J.-M. Isac, P. Travers, J. P. Santos, C. I. Szabo, A. Gumberidze, and P. Indelicato, Phys. Rev. Lett. **109**, 043005 (2012).
[54] K. Kubicek, J. Braun, H. Bruhns, J. R. Crespo López-Urrutia, P. H. Mokler, and J. Ullrich, Rev. Sci. Instrum. **83**, 013102 (2012).
[55] D. F. Anagnostopoulos, D. Gotta, P. Indelicato, and L. M. Simons, Phys. Rev. Lett. **91**, 240801 (2003).